

Impact of Experimental Parameters on Degradation Mechanism and Service Life Prediction of CFRP Anode during Simulated ICCP Process

Hongfang Sun¹, Jian Liu¹, Kun Chu¹, Shazim Ali Memon², Zhuo Cen¹, Xiaogang Zhang¹, Dawang Li¹ and Feng Xing^{1,*}

¹Guangdong Province Key Laboratory of Durability for Marine Civil Engineering,
School of Civil Engineering, Shenzhen University, Shenzhen 518060, Guangdong, P. R. China

²Department of Civil Engineering, School of Engineering, Nazarbayev University, Republic of Kazakhstan

Received: August 24, 2017, Accepted: February 20, 2018, Available online: April 27, 2018

Abstract: In actual building structure, it usually takes tens of years for the degradation to be significantly observed during impressed current cathodic protection (ICCP) process. Thus, simulated ICCP with aqueous electrolyte (instead of concrete) was used as an accelerated method to study degradation mechanism and make service life prediction. In this work, the impact of parameters including current (density) and NaCl electrolyte concentration on the degradation mechanism and service life prediction was evaluated for a simulated ICCP system with CFRP as anode. Experiments were performed with different levels of applied current (4, 10, and 20 mA) as well as with different NaCl electrolyte concentrations (3, 10, and 20% by mass). Test results showed that under all the designed conditions, both chlorination and oxidation reaction occurred during the simulated ICCP process, ensuring consistency of mechanism. From the aspect of service life prediction of CFRP, it was found that the system was not sensitive to the concentration of NaCl electrolyte but was much more influenced by the current (density) applied. Thus, for the simulated ICCP system, the current (density) should be carefully chosen since a tiny change in level of current may cause a large variation in service life prediction.

Keywords: CFRP; ICCP; Electrochemical; Degradation; Service life

1. INTRODUCTION

Corrosion of reinforcement in concrete exposed to chloride containing environments is a serious problem in civil engineering practice. Electrochemical method such as impressed current cathodic protection (ICCP) method through adjusting down the steel potential to the immunity region based on the Pourbaix diagram of iron [1], is considered to be one of the most effective and widely used approaches in controlling chloride-induced rebar corrosion.

Carbon Fiber Reinforced Polymer (CFRP), which has excellent mechanical properties, durability and ease of installation, etc., is the widely used structural reinforcement material in civil engineering [2-7]. For example, it was used as externally bonded CFRP systems in strengthening and retrofitting of reinforced concrete structural members [8-12]. In addition, CFRP's excellent conductivity and electrochemical stability makes it a potential anode materials used in ICCP [13]. Thus, researchers are focusing more in utilizing the dual functions of structural strengthening and ICCP of

reinforced concrete structures of CFRP [14-19]. For instance, Nguyen et al. investigated mechanical performance of CFRP in pre-corroded reinforced concrete beams for both structural strengthening and ICCP [20].

When ICCP process is used with concrete structure, it usually takes tens of years for degradation to be observed significantly. Thus, simulated ICCP with aqueous electrolyte instead of concrete is used to accelerate the process so that the tests can be completed within a reasonable amount of time [21, 22]. In accelerated ICCP process, the experimental parameters such as current density and concentration of electrolyte should be carefully selected as these parameters are important for maintaining consistency of mechanism as well as precisely predicting service life of CFRP anode. The factors that could affect the degradation property of anode typically include current supplied and concentration of electrolyte. From available literatures, most of the applied impressed current densities range from 2.7 to 16.7 A/m², while the concentration of NaCl electrolyte range from 1 to 20% [21-25]. The accelerated protection using an impressed current is widely being used; however, there is little information available in literature on the influ-

*To whom correspondence should be addressed:
Email: xingf@szu.edu.cn

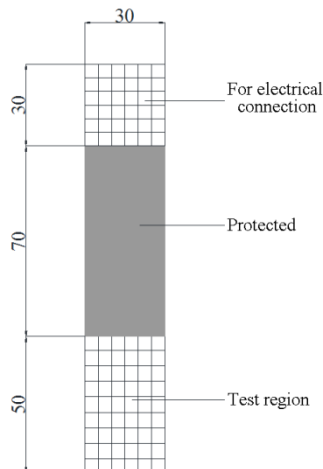


Figure 1. Geometric dimensions of CFRP specimens used for testing (unit: mm).

ence of varying the current density level and concentration of NaCl electrolyte on the effect of mechanism consistency and service life prediction of CFRP anode.

Therefore, in this research, the impact of current (density) and electrolyte concentration on the service life prediction was studied for a simulated ICCP system with CFRP as anode and NaCl solution as electrolyte. Three levels of applied current (4, 10, and 20 mA, corresponding to current density of 2.67, 6.67, and 13.33 A/m² of anode surface, respectively) and three electrolyte concentrations (3, 10, and 20% by mass) were used. The influence on cathode protection effectiveness, degradation mechanism of CFRP, and service life of CFRP anode were investigated.

2. EXPERIMENTAL

2.1. Materials

The CFRP were obtained from CA.BEN Composite Co. Ltd (Guangdong, Guangzhou province, China). The CFRP strips contained 60% volume fraction of multi-layer carbon fibers (Toray T700) and were bonded by LAM-125 / LAM-226 epoxy (Pro-Set Inc., Bay city, MI, USA). The concentration of different ingredients present in epoxy is shown in Table 1.

The geometric dimensions of tested CFRP strip are shown in Figure 1. It consist of three regions; the tested region (50 mm in length with one side exposed) having 1500 mm² of nominal anodic surface area, protected region (protected by Kafuter K-5704RTV sealant) having length of 70 mm, and electrical connection region having length of 30 mm. The thickness of CFRP used in this research was 2.00±0.01 mm.

Table 1. Chemical composition of epoxy in CFRP.

Ingredients	Concentration
Bisphenol-A type epoxy resin	37-38%
Novolac epoxy resin	19-20%
Dicyandiamide	5-6%
Methyl ethyl ketone (MEK)	36-37%

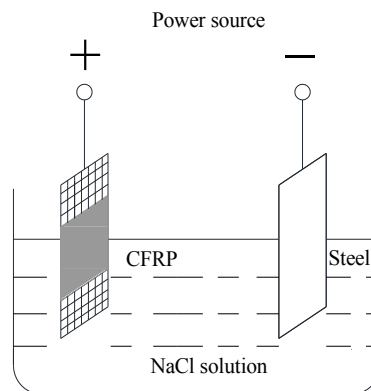


Figure 2. Details of simulated ICCP system.

2.2. Setting of simulated ICCP system and specimen designation

The details of simulated ICCP system are shown in Figure 2. It includes a CFRP strip (current anode), stainless steel strip (cathode), a constant power supply and NaCl solution (electrolyte). The spacing between anode and cathode is approximately 100 mm. Stainless steel 304 having a density of 7.9 g/cm³, elasticity modulus of 200 GPa, and thermal conductivity of 15 W/mK was used as cathode to ensure an effective electric connection. During the simulated ICCP process, constant currents of 4, 10, and 20 mA were used. These values of currents correspond to current densities of 2.67, 6.67, and 13.33 A / m² of CFRP anode surface area, respectively. As far as the electrolyte is concerned, three different concentrations of NaCl solutions (3, 10 and 20%) were used. In order to further investigate the role of current during the electrochemical process and for comparison purpose, CFRP specimens were also immersed in the 3, 10, and 20% NaCl solutions without current applied as control samples. The testing was carried out for 21 days. The details of experimental matrix are shown in Table 2.

Table 2. Details of experimental matrix.

Group	Specimen identification	Current (mA)	Current density (A/m ²)	Concentration of NaCl solution (%)
S3	I0S3	0	0	3
	I4S3	4	2.67	3
	I10S3	10	6.67	3
	I20S3	20	13.33	3
S10	I0S10	0	0	10
	I4S10	4	2.67	10
	I10S10	10	6.67	10
	I20S10	20	13.33	10
S20	I0S20	0	0	20
	I4S20	4	2.67	20
	I10S20	10	6.67	20
	I20S20	20	13.33	20

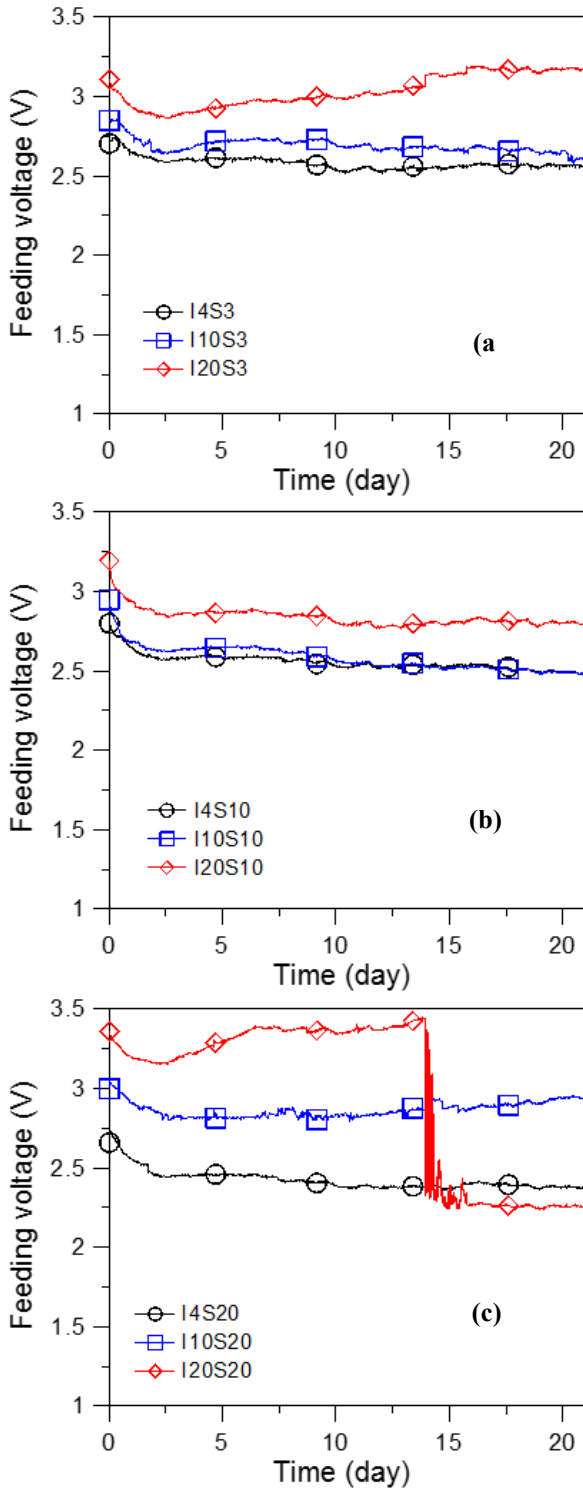


Figure 3. Feeding voltage during simulated ICCP process with different NaCl concentrations and applied currents.

The specimens were designated according to level of applied current and concentration of NaCl solution. For example, in I10S20, 'I10' represents the nominal applied current of 10 mA while S20 represents 20% concentration of NaCl solution.

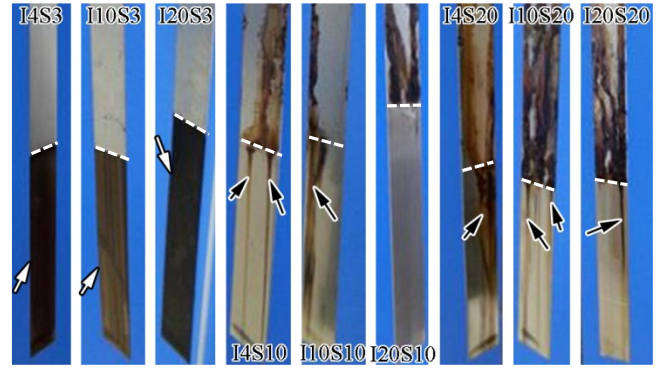


Figure 4. Surface of steel cathodes after simulated ICCP process. The white arrows indicate the attachment of carbon black from solution. The black arrows indicate the dissolved rust trace from the part above the electrolyte surface. The dashed lines separate the part immersed in solution and that exposed to air.

2.3. Testing methods

In this research, the feeding voltage measurements, XRD, and FTIR were conducted to investigate the degradation mechanism of CFRP anode and its influence on service life prediction. For each test, two samples were used to ensure the repeatability.

2.3.1. Feeding voltage

During simulated ICCP process, the connection of the circuit was evaluated by the feeding voltage between stainless steel and CFRP. The feeding voltage was monitored with a multi-channel data logger at an interval of 1 min.

2.3.2. XRD

The mineralogy of CFRP surface was evaluated by taking XRD measurements using Bruker D8 instrument with CuK α source operated at 40 kV and 40 mA. For XRD measurements, the sample was cut to approximately 20 * 13 mm² size while the phase identifying analysis was performed using the software available with the instrument.

2.3.3. FTIR

Perkin-Elmer FTIR spectrometer was used to evaluate the degradation mechanism of CFRP in different solutions. For sample preparation, CRFP was mixed with KBr in controlled humidity environment. After that, the mixed sample was pressed and pellets were used to obtain infrared spectrum via Spectrum Version 5.0.1. Following scanning parameters were used: range 400-4000 cm⁻¹, resolution 2 cm⁻¹, and number of scans equal to 16.

3. TEST RESULTS AND DISCUSSION

3.1. Protection effectiveness of cathode

3.1.1. Feeding voltage

During simulated ICCP process which continued for 21 days, the feeding voltages between CFRP anode and stainless steel cathode with different concentration of NaCl solution and applied current was monitored and the results are shown in Figure 2. At all given conditions, the feeding voltages remained stable between 2.4 and

UNCORRECTED PROOF

UNCORRECTED PROOF

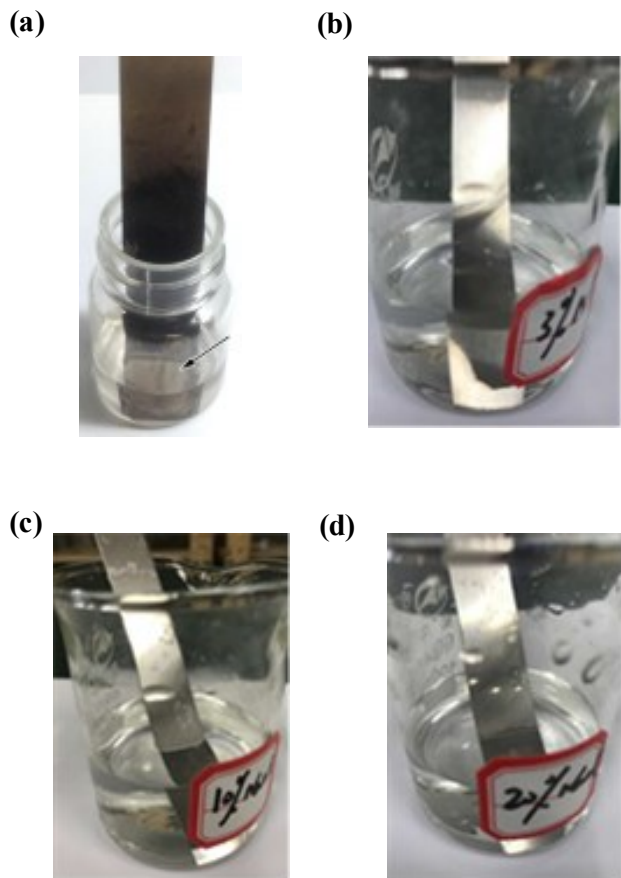


Figure 5. The removal of carbon black attached to the surface of steel cathode (a) and steels immersed in different concentrations of NaCl solution after 21 days with applied current of 0 mA; (b) 3% NaCl solution; (c) 10% NaCl solution; (d) 20% NaCl solution.

3.5 V. It indicates that during the tested period, the circuit can provide a continuous protection to the cathode. Furthermore, it suggests that at all the testing conditions (currents of 4-20 mA and concentrations of NaCl solutions of 3-20%); the conductivity of solutions is much higher than that of CFRP anode. This means that the feeding voltage was mainly determined by CFRP and the change of feeding voltages was caused by CFRP. For the specimen with 20% NaCl concentration and applied current of 20 mA, a sudden drop in feeding voltage at the age of 14 day was observed (Figure 4 (c)). This may be attributed to the increase in contact area between the carbon fibers because of corrosion and removal of epoxy matrix in CFRP. However, it did not affect the connection through the circuit and the cathode was protected. Therefore, at the given NaCl concentration and level of applied current, the cathode can be applied a continuously cathode protection during 21 days electrochemical process.

3.1.2. Evaluating the surface of cathode

After 21 days of electrochemical process, the surface of steel cathode was monitored and the results are presented in Figure 4. For S3 group having 3% NaCl concentration, the surface of sample

above the solution was clean and no corrosion was observed. However, the sample surface immersed in solution showed darker color and the color slightly varied for different currents (Figure 4, white arrow). The color may be attributed to carbon black from solution, which originated from the corrosion of CFRP. However, this color can easily be removed from the surface by immersing the sample in water as shown in Figure 5 (black arrow). Moreover, when carbon black was removed, the exposed steel surface exhibited no sign of corrosion. Hence for the tested feeding voltage (Figure 3), it seems that the layer of carbon black does not influence the conductivity of the system. It can therefore be deduced that during the cathode protection process, S3 group can maintain a stable electrical connection. When the concentration of NaCl electrolyte increased to 10% (S10) and 20% (S20), the part of steel sample immersed in solution showed no sign of corrosion as well as no adherence of carbon black. However, corrosion was observed in the part of steel sample above the solution as this part was not electrochemically protected. Moreover, corrosion was more severe in S20 than S10. It is believed that the corrosion products dissolved by moisture were carried down to the protected region (as indicated by black arrows in Figure 4) suggesting that corrosion tends to occur in the area close to the highly-concentrated NaCl solution with high environmental humidity.

In order to further investigate the role of current during the electrochemical process and for comparison purpose, steels were also immersed in the 3, 10, and 20% NaCl solutions without current applied for 21 days. The results are presented in Figures 5 (b)-(d). It can clearly be seen that neither steel nor color of solutions changed suggesting that the current applied plays an important role during electrochemical process. However, by comparing the three cathodes applied with different current levels and under the same NaCl concentration, it can be seen that during the electrochemical process, the influence of current level seems insignificant.

Based on above results, it can be concluded that for a current level in between 4-20 mA (current density 2.67-13.33 A/m²), the cathode of the system was well protected. However, higher concentration of NaCl electrolyte (such as 10-20%) will lead to corrosion of steels or iron connecting wires close to the surface of aqueous solution and in turn may influence the effectiveness of the experiment operated for a long duration. Hence, from this aspect, the lower concentration of NaCl such as 3% is preferred unless the system is fully protected.

3.2. Degradation mechanism of CFRP anode

The degradation mechanism of CFRP in different concentrations of NaCl solution was evaluated using XRD and FTIR techniques as described in the following sections.

3.2.1. XRD

XRD technique was used to determine the mineralogy of degraded CFRP specimens. The XRD spectra obtained after electrochemical process are shown in Figure 6. NaCl was the only crystalline phase observed in the XRD spectra and came from the NaCl electrolyte. As expected, more NaCl was formed with the increase of concentration of NaCl solution as well as with the increase in the level of applied current. The latter may be related to the movement and precipitation of negative chloride ion towards CFRP anode during the simulated ICCP process. The broad amorphous humps

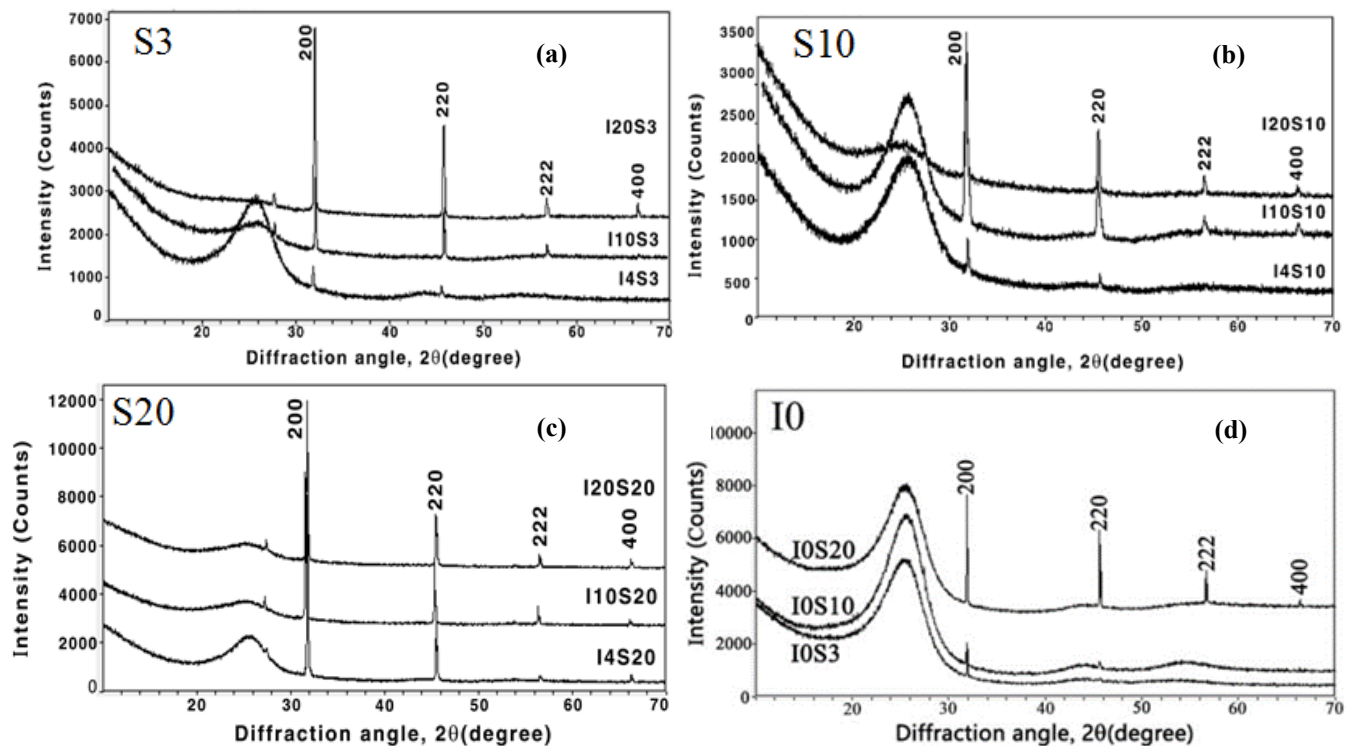


Figure 6. XRD of CFRP anode surface obtained in different concentrations of electrolyte solutions and currents. (a) 3% NaCl solution; (b) 10% NaCl solution; (c) 20% NaCl solution; (d) Control specimens with applied current of 0 mA. The indexed crystalline phase was identified to be NaCl.

can also be seen in the XRD spectra which are believed to be related to carbon fiber and residue epoxy. Furthermore, for all the solution levels, the height of amorphous humps decreased with increase in the level of applied currents, indicating that more CFRP was consumed at higher current.

From above discussion, it is inferred that for different concentrations of NaCl solution and applied current levels, the crystalline phases observed in XRD spectra of CFRP were from crystallized NaCl electrolyte rather than the degradation products of CFRP anode, and it thus could not reflect the degradation mechanism of CFRP anode. We would like to mention here that due to the limitation of XRD technique, the information regarding amorphous phases present in corroded CFRP cannot be detected. Therefore, FTIR technique was used to carry out further investigation to find out the degradation mechanism at different NaCl concentrations and applied current levels.

3.2.2. FTIR

The FTIR spectra of specimens with different concentrations of NaCl solution and applied current levels are shown in Figure 7 while the significant peaks are indicated by arrows. Compared with as-received CFRP, the spectra of control CFRP specimens immersed in different concentrations of NaCl solutions and without current applied showed almost no change (Figure 7d). For as-received CFRP, the bands at 1506 and 830 cm^{-1} , which were attributed to the stretching vibration of benzene in the epoxy structure [26-28], were observed. These bands decreased or even disap-

peared with the increase in current density indicating that the benzene ring might have opened when CFRP acted as an anode. In as-received CFRP spectra, the band at 1181 cm^{-1} , which represent the C-N stretching in epoxy [29, 30], can also be observed. The decrease in C-N peak with increase in current density indicates that the linkage between epoxy resins is broken and is the potential main cause of epoxy degradation. One of the choices of the open carbon linkage could be related to the re-bonding of Cl, which is confirmed by newly formed C-Cl stretching peak at 804 cm^{-1} [31, 32]. For the specimens subjected to electrochemical process, the peaks at 1732, 1697, 1472, 1454, 1394, 1273, and 935 cm^{-1} can be observed. The intensity of 1732, 1697, and 1394 cm^{-1} bands belong to C=O stretching of carbonyl group, ester, and COO^- group, respectively [26, 33-36]. The bands of 1472 and 1454 cm^{-1} belong to methoxy groups [37] while the signals at 1273 and 935 cm^{-1} are ascribed to the stretching and vibration of C-O-C bond [38-41]. The common characteristic of these four bands (1472, 1454, 1273, and 935 cm^{-1}) is oxygen related, which is believed to be the second choice for open carbon linkage. The presence of these bands indicates that during the simulated ICCP process, more oxidation reaction of epoxy occurred. Meanwhile, in the as-received spectra, the presence of 1047 cm^{-1} band (C-OH of diglycidyl ether unit [26]) decreased with the level of applied current implying that condensation reaction occurred to form those oxygen-related bonds.

By analyzing FTIR spectra, it can be seen that for a certain NaCl concentration such as 3%, when the current increased from 0 to 4 mA, both chlorination and oxidation reaction appeared. However,

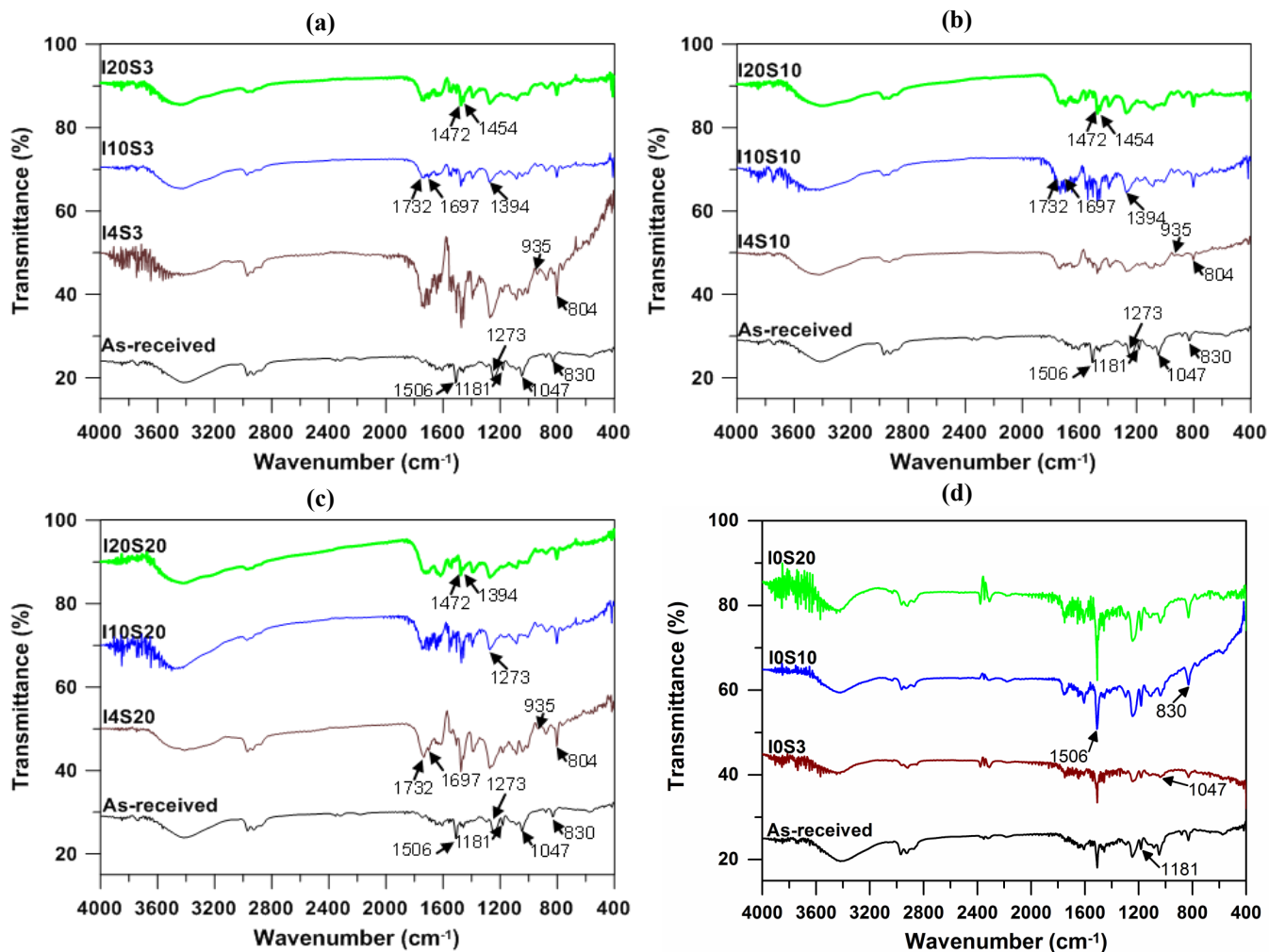


Figure 7. FTIR spectra of CFRP in different concentrations of the NaCl solutions and currents. (a) 3%; (b) 10%; (c) 20%. (d) The FTIR spectra of control CFRP specimens with applied current of 0 mA.

when the current increased from 4 to 10 and 20 mA, no significant change in FTIR spectra was observed. The same is also true for NaCl concentration increased from 3% to 10% and 20% at a certain current level. However, the quantity of degradation products might vary and was not reflected here due to the resolution limit of this technique. In conclusion, both chlorination and oxidation reaction occurred during the simulated ICCP process in NaCl solution. However, in the current range 4 to 20 mA and NaCl concentration range 3 to 20%, the degradation mechanism of CFRP anode is similar.

3.3. Service life prediction of CFRP anode

3.3.1. Degradation depth

In order to assess the service life of CFRP in NaCl solution during simulated ICCP process, the degradation depth of CFRP was measured. The CFRP showed no significant change after immersing in 20% NaCl solution for 21 days without current applied (Figure 8b). However, three parts (soft part, hard but laminating part, and un-damaged part) were obtained when the CFRP sample

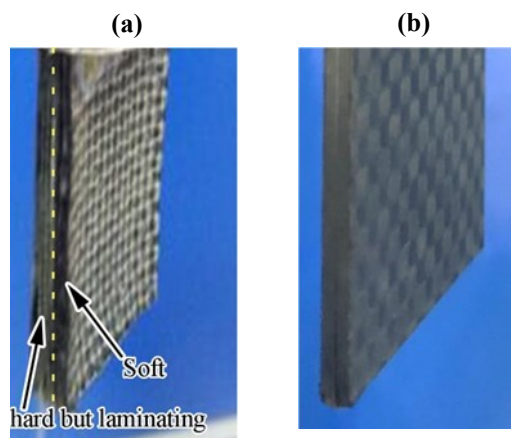


Figure 8. (a) Degradation pattern of CFRP after simulated ICCP process showing two parts (soft and hard but laminating part) as indicated by arrows. (b) CFRP after immersing in 20% NaCl solution for 21 days without current applied.

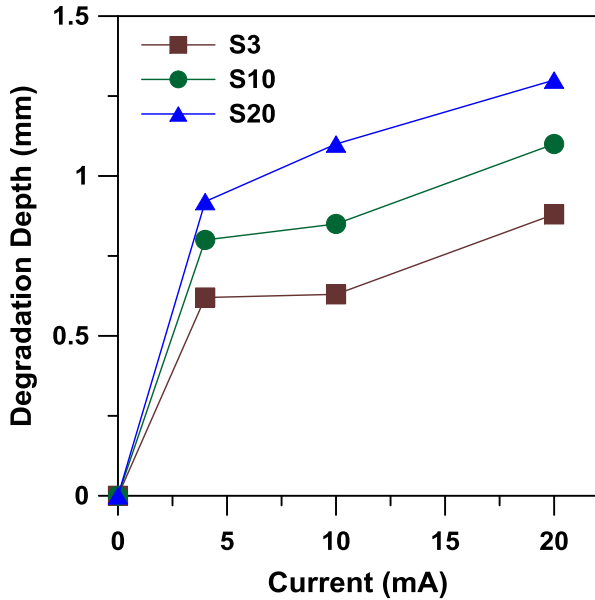


Figure 9. Degradation depth of CFRP with different solution concentrations and applied currents.

was immersed in NaCl solutions and subjected to different level of applied current. In the soft part, the epoxy was weak and corroded and can easily be removed by knife through scraping (Figure 8a). In the hard but laminating part, the epoxy in a specific layer seems un-damaged but the epoxy between adjacent layers was corroded (Figure 8a). This part was difficult to remove by scraping. However, it can be removed layer by layer by peeling. We would like to mention here that these two parts were counted towards degradation depth. Finally, the un-damaged part was hard and could not be removed by either scraping or peeling. The thickness of this part was measured and used to calculate the degradation depth through formula (the total thickness – un-damaged part).

The results of degradation depths of CFRP in varied NaCl concentrations and applied current levels are shown in Figure 9. It can be seen that the degradation depth increased with the increase in the level of electrolyte concentration as well as applied current

level, since at these conditions more oxidizing species (chloride and oxygen) will be produced at the anode region. For a certain applied current level (4 or 10 or 20 mA), the degradation depth increased with increasing concentration of NaCl electrolyte (from 3% to 20%). This shows that the higher solution concentration increased the degradation depth. As far as degradation rate is concerned, the degradation depths increased firstly at a faster rate followed by gradual increase. For a certain NaCl concentration, when the current level increased from 0 to 4, 10, and 20 mA, it can also be seen that when NaCl concentration increased from 3% to 10% and 20%, the change in degradation depths is relatively small (0.62-0.88 mm for current 4 mA, 0.80-1.10 for current 10 mA, and 0.92-1.30 for current of 20 mA). It indicates that the existence of currents and chloride has an important impact on the degradation of CFRP anode. However, when the current level increased from 4 to 20 mA and the concentration of NaCl solution from 3% to 20%, the impact on the degradation of CFRP is much less. The finding is consistent with the conclusion of FTIR analysis presented in Section 3.3.2. Finally, the degradation rate was calculated by applying the following formula (degradation depth / duration time) and the results are presented in Table 3. The degradation rate varied from 29.52 and 61.90 $\mu\text{m}/\text{day}$. Accordingly, the service life of the CFRP strip was estimated as discussed in next section.

3.3.2. Service life estimation

The NACE standard [42] was used to determine the service life of CFRP anode. As per standard, for CFRP to survive for 40 years at a current density 108 mA/m², the estimated total charge density is 38500 A-h/m² of anode surface. This current density is commonly used for reinforced concrete structures deteriorated by corrosion [43]. For example, for the specimen in 3% NaCl solution and with applied current 4 mA (during 21 days simulated ICCP test), a total charge density of approximately $2.67 \times 21 \times 24 = 1346$ A-h/m² passed through the interface with 0.62 mm CFRP corroded. This means that the whole CFRP having thickness of 2.00 mm can survive charge density of $1346 \times 2.00 / 0.62 = 4342$ A-h/m² and represents a service life of $4342 / 38500 \times 40 = 4.51$ years. According to the calculations (Table 3), the service life of tested specimens varied from 3.04 to 15.86 years. It is worth mentioning here that in comparison to aqueous solutions, the aggressiveness of corrosion on CFRP in real reinforced concrete structure would be less due to much less electrolyte in pores of concrete. Hence, in actual structure, CFRP

Table 3. Degradation rate and service life calculation for CFRP anode.

Group	Specimen identification	Current (mA)	Current density (A/m ²)	Degradation depth (mm)	Degradation rate ($\mu\text{m}/\text{day}$)	Service life (year)
S3	I4S3	4	2.67	0.62	29.52	4.51
	I10S3	10	6.67	0.63	30.00	11.09
	I20S3	20	13.33	0.88	41.90	15.86
S10	I4S10	4	2.67	0.80	38.10	3.50
	I10S10	10	6.67	0.85	40.48	8.22
	I20S10	20	13.33	1.10	52.38	12.69
S20	I4S20	4	2.67	0.92	43.81	3.04
	I10S20	10	6.67	1.10	52.38	6.35
	I20S20	20	13.33	1.30	61.90	10.74

may survive much longer than the estimates given here for electrochemical condition.

In order to determine the influence of NaCl electrolyte concentration on the service life of CFRP, Table 3 is referred. It can be seen that for applied current of 4 mA, when the concentration of NaCl electrolyte increased from 3% to 10% and 20%, the calculated service life decreased from 4.51 years to 3.50 (22.5% decrease) and 3.04 years (32.6% decrease). It indicates that for 1% change of concentration from 3% to 10%, the predicted service life changed by 9.64% while for 1% change of concentration from 3% to 20%, the predicted service life changed by 5.75%. Similarly, for currents of 10 mA, a 1% change of NaCl electrolyte concentration from 3% to 10% and from 3% and 20%, the predicted service life changed by 11.09 and 7.54% respectively. In the same way, for currents of 20 mA, the changes are 8.57 and 5.70% respectively.

The influence of applied current level on service life of CFRP anode was also determined. It can be seen that for 3% NaCl concentration, when the current level increased from 4 mA to 10 and 20 mA, the predicted service life increased from 4.51 years to 11.09 (146% increase) and 15.86 (252% increase) years. It indicates that for 1% change of applied current level from 4 mA to 10 mA, the predicted service life changed by 97% while for 1% change of applied current level from 4 mA to 20 mA, the predicted service life changed by 59%. Similarly, for 10% NaCl concentration, a 1% change of current from 4 mA to 10 mA and from 4 mA to 20 mA, the predicted service life changed by 90 and 66% respectively. The changes for concentration of 20% are 73 and 63% respectively.

From the above calculation and for the tested conditions, it can be concluded that the predicted service life of CFRP in simulated electrochemical system is not sensitive to the concentration of NaCl electrolyte (change less than 12%). However, it is more influenced by the current applied (change more than 60%). Hence, for the simulated ICCP system, the current (density) should be carefully chosen since a tiny change in level of current may cause a large variation in service life prediction.

4. CONCLUSIONS

In this research, the impact of current (density) and NaCl electrolyte concentration on the service life prediction for simulated ICCP system with CFRP as anode was investigated. Based on the test results, the following conclusions can be drawn.

1) From the aspect of cathodic protection, a stable connection was maintained during the simulated ICCP and the cathode of the system was well protected. However, higher concentration of NaCl electrolyte (such as 10-20%) will lead to corrosion of steels or iron connecting wires close to the liquid surface unless the whole system is fully protected. Hence, from this aspect, the lower concentration of NaCl such as 3% is preferred unless the system is fully protected.

2) Under all the designed conditions, both chlorination and oxidation reaction occurred during the simulated ICCP process, ensuring consistency of mechanism.

3) It was found that the predicted service life of CFRP in simulated ICCP system is not sensitive to the concentration of NaCl electrolyte (change less than 12%). However, it is more influenced by the current applied (change more than 60%). Hence, for the simulated ICCP system, the current (density) should be carefully

chosen since a tiny change in level of current may cause a large variation in service life prediction.

Besides the current and concentration of NaCl electrolyte, power-on time is another important factor which should be investigated to improve the accuracy of service life prediction of CFRP anode. Based on the findings of this work, the trend of service life with power-on time can be evaluated in future research.

5. ACKNOWLEDGEMENTS

The research work described in this paper was supported by the Chinese National Natural Science Foundation (Grant Nos. 51520105012, 51678368, and 51508338), the (Key) Project of Department of Education of Guangdong Province (Grant No. 2014KZDXM051), and the High Calibre Overseas Talents Scheme of the Municipal Government of Shenzhen (Grant No. 000114). We also thank the Guangdong Provincial Key Laboratory of Durability for Marine Civil Engineering, College of Civil Engineering, Shenzhen University for providing facilities and equipments.

REFERENCES

- [1] M. Pourbaix. *Atlas of electrochemical equilibria in aqueous solutions*, National Association of Corrosion Engineers, Houston, Tex., United States (1974).
- [2] ACI 562M-13. Code Requirements for Evaluation, Repair and Rehabilitation of Concrete Buildings and commentary, in, American Concrete Institute, MI, United States (2013).
- [3] BS EN 1504-4. Products and systems for the protection and repair of concrete structures - Definitions, requirements, quality control and evaluation of conformity - Part 4: Structural bonding, in, British Standards Institute London (2004).
- [4] M. Karantzikis, C. G. Papanicolaou, C. R. Antonopoulos and T. C. Triantafyllou. *Journal of Composites for Construction*, 9, 480 (2005).
- [5] T. C. Rousakis. *Journal of Composites for Construction*, 17, 732 (2013).
- [6] T. C. Rousakis and I. S. Tourtouras. *Composites Part B: Engineering*, 58, 573 (2014).
- [7] Y. Li, X. Liu and M. Wu. *Construction and Building Materials*, 134, 424 (2017).
- [8] R. A. Hawileh, M. Z. Naser and J. A. Abdalla. *Composites Part B-Engineering*, 45, 1722 (2013).
- [9] V. J. Ferrari, J. B. de Hanai and R. A. de Souza. *Construction and Building Materials*, 48, 485 (2013).
- [10] J. P. Firmo, J. R. Correia and P. Franca. *Composites Part B: Engineering*, 43, 1545 (2012).
- [11] R. A. Hawileh, M. Z. Naser and J. A. Abdalla. *Composites Part B: Engineering*, 45, 1722 (2013).
- [12] Y. Li, X. Liu and J. Li. *Journal of Materials in Civil Engineering*, 29, 04016275 (2016).
- [13] M. Raupach, B. Elsener, R. Polder and J. Mietz. *Corrosion of reinforcement in concrete: mechanisms, monitoring, inhibitors and rehabilitation techniques*, CRS Press, Boca Raton, Boston New York, Washington, DC (2007).
- [14] F. Lee-Orantes, A. Torres-Acosta, M. Martínez-Madrid and C.

- López-Cajún. ECS Transactions, 3, 93 (2007).
- [15] S. Gadve, A. Mukherjee and S. N. Malhotra. *Aci Materials Journal*, 107, 349 (2010).
- [16] C. Van Nguyen, P. Lambert, P. Mangat, F. O'Flaherty and G. Jones. *ISRN Corrosion*, 814923 (9 pp.) (2012).
- [17] S. Gadve, A. Mukherjee and S. N. Malhotra. *Corrosion*, 67, 1 (2011).
- [18] P. Lambert, C. Van Nguyen, P. S. Mangat, F. J. O'Flaherty and G. Jones. *Materials and structures*, 48, 2157 (2015).
- [19] Y. Li, X. Liu, M. Wu and W. Bai. *Construction and Building Materials*, 153, 436 (2017).
- [20] C. V. Nguyen, P. S. Mangat, P. Lambert, F. J. O'Flaherty and G. Jones. in *3rd International Conference on Concrete Repair, Rehabilitation and Retrofitting, ICCRRR 2012, September 3, 2012 - September 5, 2012*, p. 1179, Concrete Repair, Rehabilitation and Retrofitting III - Proceedings of the 3rd International Conference on Concrete Repair, Rehabilitation and Retrofitting, ICCRRR 2012, Cape Town, South Africa (2012).
- [21] H. Sun, S. A. Memon, Y. Gu, M. Zhu, J.-H. Zhu and F. Xing. *Materials and Structures*, 49, 5273 (2016).
- [22] H. Sun, L. Wei, M. Zhu, N. Han, J.-H. Zhu and F. Xing. *Construction and Building Materials*, 112, 538 (2016).
- [23] H. F. Sun, G. P. Guo, S. A. Memon, W. T. Xu, Q. W. Zhang, J. H. Zhu and F. Xing. *Composites Part a-Applied Science and Manufacturing*, 78, 10 (2015).
- [24] J. H. Zhu, M. C. Zhu, N. X. Han, W. Liu and F. Xing. *Materials*, 7, 5438 (2014).
- [25] H. Q. Yang, Y. Wang, S. S. Tu, Y. M. Li and Y. Huang. *International Journal of Electrochemical Science*, 11, 3238 (2016).
- [26] Y. Wang, X. Cui, H. Ge, Y. Yang, Y. Wang, C. Zhang, J. Li, T. Deng, Z. Qin and X. Hou. *ACS Sustainable Chemistry & Engineering*, 3, 3332 (2015).
- [27] S. T. Cholake, M. R. Mada, R. K. S. Raman, Y. Bai, X. L. Zhao, S. Rizkalla and S. Bandyopadhyay. *Defence Science Journal*, 64, 314 (2014).
- [28] B. I. Kharisov, O. V. Kharissova and U. O. Méndez. *Radiation synthesis of materials and compounds*, CRC Press, Boca Raton, FL (2013).
- [29] Z. P. Zhang, Y. Lu, M. Z. Rong and M. Q. Zhang. *RSC Advances*, 6, 6350 (2016).
- [30] F. Huang, F. Huang, Y. Zhou and L. Du. *Polymer journal*, 42, 261 (2010).
- [31] X. Jing, F. Liu, X. Yang, P. Ling, L. Li, C. Long and A. Li. *Journal of hazardous materials*, 167, 589 (2009).
- [32] <http://www.chem.ucalgary.ca/courses/351/Carey5th/Ch13/ch13-ir-2.html>, in.
- [33] <https://theses.lib.vt.edu/theses/available/etd-32398-61326/unrestricted/11-.pdf>, in.
- [34] N. D. Mailhot, S. Morlat-Therias, P. O. Bussiere and J. L. Gardette. *Macromolecular Chemistry and Physics*, 206, 585 (2005).
- [35] R. Zhang. Novel conductive adhesives for electronic packaging applications: A way towards economical, highly conductive, low temperature and flexible interconnects, in *School of Chemistry and Biochemistry*, Georgia Institute of Technology (2011).
- [36] V. M. Litvinov and P. P. De. *Spectroscopy of rubbers and rubbery materials*, Rapra Technology Ltd, Shawbury (2002).
- [37] E. V. Steen, L. H. Callanan and M. Claeys. *Recent Advances in the Science and Technology of Zeolites and Related Materials: Proceedings of the 14th International Zeolite Conference, Cape Town, South Africa, 25-30th April 2004*, Elsevier Science & Technology Books (2005).
- [38] S. Maharubin. Infrared spectroscopy measurements of native and functionalized poly (vinyl alcohol) nanowebs, in *Analytical Chemistry*, Texas Tech University (2015).
- [39] P. Pařík, S. Šenauerová, V. Lišková, K. Handlř and M. Ludwig. *Journal of heterocyclic chemistry*, 43, 835 (2006).
- [40] D. Montarnal. Use of reversible covalent and non-covalent bonds in new recyclable and reprocessable polymer materials, in *Polymers*, <https://tel.archives-ouvertes.fr/pastel-00694348/document> (2011).
- [41] N. P. Bansal, J. P. Singh, S. Ko, R. Castro, G. Pickrell, N. J. Manjooran, M. Nair and G. Singh. *Processing and Properties of Advanced Ceramics and Composites V: Ceramic Transactions*, Wiley-American Ceramic Society (2013).
- [42] N. S. TM0294. NACE International: Houston, TX, USA (2007).
- [43] BS EN ISO 12696: Cathodic Protection of Steel in Concrete, in *British Standards Institution*, British Standards Institution, London (2012).

